DRYING TECHNOLOGY
https://doi.org/10.1080/07373937.2023.2261049

Taylor & Francis
Taylor & Francis Group

Radial Jet Reattachment impingement drying of corn tortillas

Juan Rodríguez-Ramírez[a,b], Milad Farzad[a], Zahra Noori O'Connor[a], and Jamal Yagoobi[a]

[a]Center for Advanced Research in Drying, Worcester Polytechnic Institute, Worcester, MA, USA; [b]Instituto Politécnico Nacional, CIIDIR Oaxaca, Ciudad de Mexico, México

ABSTRACT

This study evaluates the heat and mass transfer behavior of innovative Radial Jet Reattachment (RJR) nozzles to analyze the texture and color characteristics of crispy tostadas. A new experimental method for measuring steady-state evaporation is proposed and validated to determine the averaged coefficients of convective heat and mass transfer for different drying conditions and geometrical parameters of RJR nozzles. The experiment is designed using a 2^4 factorial design approach. The factors that are considered include nozzle exit angle (10° and 45°), tortillas thicknesses (1.03 mm and 1.66 mm), air drying temperature (200 °C and 250 °C) and air mass flow rate (17.0 m^3/h and 27.2 m^3/h). The findings indicate that for the impingement drying of tortillas, it is crucial to consider convection and diffusion as the primary factors in selecting the appropriate operating conditions. Moreover, the study concludes that the RJR nozzle with a 45° exit angle exhibits a higher drying rate than the RJR nozzle with a 10° exit angle. The study found that neither the type of nozzle nor the air drying conditions had a significant impact ($\alpha \leq 0.05$) on the texture and color of the final product. The utilization of RJR nozzles for impinging drying of tortillas is a promising and robust process that enables the production of crispy tostadas without negatively impacting the quality characteristics of the final product.

ARTICLE HISTORY
Received 9 December 2022
Revised 20 August 2023
Accepted 13 September 2023

KEYWORDS
Impingement drying; innovative nozzles; heat and mass transfer; food quality; RJR nozzle

Introduction

In order to promote a healthy society, it is necessary to offer foods that are low in fat, gluten-free, high in fiber with desirable texture and flavor characteristics.[1] "Tortilla" is the name of a Mexican product prepared by cooking a "nixtamalized disk of corn dough" on a smooth, flat griddle. "Unfried tostada" is a healthy product made from a dried-up or baked tortilla that becomes dehydrated and crunchy. This process ensures that the material can be preserved for several weeks without refrigeration and without spoiling. Additionally, these products do not require non-oxidative atmospheres like fried products do. The fragility of the 'Tostadas' represents a challenge in their production, packaging, transportation, and marketing.

The consumption of tortillas has experienced tremendous worldwide growth, both as a dietary diversification among all ethnic groups and as a healthier alternative to other types of bread. The food industry has attempted to simplify the manufacturing process by utilizing instant flours and specialized machines, such as three-tier gas-fired oven conveyor belts.[2] Preparing dried or baked tortillas requires technology to achieve a uniform product with acceptable quality characteristics. Cooking, drying, baking, and toasting tortillas and other similar products can be integrated into a single technology in the food industry, resulting in energy and material savings. Such an approach can also help in reducing capital and investment costs while ensuring acceptable product quality characteristics for both producers and consumers.

Impingement drying has shown promise as a technology suitable for integration into continuous processes where the food material is transported by conveyor belts. Mujumdar and Tsotsas[3,4] reviewed the state of the art of modern Drying technologies. They provided a comprehensive review of the effect of various parameters in drying with impinging jet nozzles. The most important applications of impingement jet are processes where materials resist fluid impacts, such as annealing metal and plastic sheets, glass tempering, and drying textiles, sheet metal, paper, and film material. Impingement flow devices allow short flow paths at the surface and, therefore, relatively high heat transfer rates.[3,4] The advantage of impingement dryers lies in their high evaporative capacity, which is

CONTACT Juan Rodríguez-Ramírez jrodrigr@ipn.mx

due to the high temperatures and air flow rates they utilize. The design of an impingement dryer takes into account the geometrical parameters, operating conditions, and material characteristics to be dehydrated, which can either be specified or chosen arbitrarily. The challenging aspect is to choose a system that can provide the best balance between energy consumption, production capacity, and product quality.[5]

Impingement dryers are suitable for food processing because they can quickly dry or bake foods, particularly those that require exposure to high temperatures for a short duration.[6] After all, increased flow and heat transfer rates in impingement dryers can degrade heat-sensitive food products. The deterioration of food during drying and other thermal treatments is dependent on the time-temperature combination. Even when the temperature is high, if the time of exposure is short, the deterioration may be less. Therefore, when designing an impingement dryer for food, experimental drying data should be considered to ensure optimal results. Lujan-Acosta et al.[7] used impingement drying to dry a circled-shape (5.08 cm in diameter) raw tortilla chip. The air temperature mainly affected the product's microstructure and texture. A smoother and tighter microstructure and crispier chips were obtained at high temperatures. Banooni et al.[8] studied the influence of airflow and temperature variation on bread temperature, weight loss, thickness, and surface color of baked flat bread. They concluded that impingement ovens could be used successfully instead of direct fire ovens in flat bread bakeries. Farzad and Yagoobi[9] showed that the impingement drying with modified nozzles produced dried apple slices with less color deterioration and fewer nutritional losses compared to drying with conventional nozzles.

Impinging nozzles are essential components of impingement systems, which typically include perforated, in-line jets (ILJ), and slot jet (SJ) nozzles. Farzad et al.[9,10] extensively discuss published experimental and numerical studies that investigate the performance of various types and geometrical configurations of impingement nozzles. The effect on the pattern, topology, behavior, and performance of the turbulent flow, local and average heat transfer, transport characteristics of various geometrical parameters; shape, hydraulic diameter, configuration, inclination, arrays of the nozzles, as well as surface to nozzle spacing, surface motion, surface roughness, temperature, and mass rate of the fluid.

Although significant advances are being made in understanding transport phenomena under jets, the design remains empirical, mainly when the flow rates and temperature are increased to achieve high heat and mass transfer coefficients without damaging the product, especially for moist fragile surfaces and heat-sensitive materials like food. Two innovative impingement jet nozzles are the radial and slot jet reattachment nozzles, RJR, and SJR, respectively.[11,12] In reattachment nozzles, the fluid stream is directed outward to a point where it separates from the nozzle into a free stream. The turbulent viscous mixing that occurs at the boundaries of this stream induces secondary flow by mass entrainment.[13] When placed near a surface, the induced flow from the lower edge of the jet stream creates a low-pressure region beneath the nozzle. The low-pressure region forces the jet stream to turn down until the stream impinges, or reaches, the plate in a circular (for RJR) or an oval (for SJR) shape centerer underneath the nozzle.[14] The stream, now reattached to the surface of the flat plate, divides. Part of the stream turns radially outward, and the remainder radially inward. This process results in a highly turbulent reattachment ring.[15] The intense turbulence associated with this phenomenon is mainly responsible for the high heat and mass transfer between the fluid and the impingement/reattachment surface.[16,17]

The characteristic flow pattern of the RJR and SJR also provides another unique feature. The magnitude and direction of the net force exerted by the fluid on the reattachment surface can be controlled. Zero and even negative net forces can be attained with different designs of the RJR nozzle.[12] Specifically, the flow exit angle can be used to manage the force direction on the impingement surface. Such characteristics allow high heat and mass transfer coefficients without damaging the reattachment surface.[11–17]

Knowledge of the dependence of external variables and material characteristics on the heat and mass transfer rate is necessary to choose the best system in terms of effectiveness and energy efficiency. Convective heat and mass transfer coefficients can be estimated from empirical correlations. Martin[18] developed empirical equations to estimate the local and heat and mass transfer for a single and an array of in-line jets (ILJ) and slot jet (SJ) nozzles. The RJR and SJR nozzles are geometrically more complex and produce a reattachment flow pattern. Narayanan et al.[19] developed a correlation for a peak (reattachment) heat transfer coefficient for slot jet reattachment (SJR) nozzles. The influence of turbulence and geometric variations may cause much of the scatter of data, making it difficult to obtain equations for

predicting mass and heat transfer coefficients. Farzad et al.[9] quantified local heat transfer coefficients generated by RJR, SJR and ILJ nozzles for all the test conditions, measuring heat flux using a data logger connected to a heat flux sensor.

This work proposes a simple experimental method to evaluate the average mass and heat transfer coefficients for all the conditions explored. It involves measuring the average surface temperature and weight loss under steady-state evaporation in a water-saturated porous stone with a diameter similar to that of the samples considered in this study.

In impinging drying using RJR nozzles, it is crucial to understand systematically how food products are affected by the turbulent flow and intensive heat treatment. The exit angle of the RJR can influence flow characteristics and increase heat and mass transfer coefficients without compromising the quality of the dried tortillas. In this experimental study, two Radial Jet Reattachment (RJR) nozzles with exit angles of 10° and 45° under different air-drying conditions are considered.

The success of integrating impingement drying with reattachment nozzles into the continuous cooking, drying, and baking process of tortillas depends on the drying performance and final quality characteristics of the baked products. The objective of this study is to evaluate the moisture transport characteristics and quality of dehydrated tortillas of two thicknesses using RJR nozzles. The convective heat and mass transfer coefficients, as well as diffusivity, were experimentally calculated to determine the drying rate and to evaluate the effect of this method on the color and texture of the baked tortillas.

Materials and methods

Tortilla preparation

Tortillas were made from nixtamalized flour (Maseca®), water and salt. The dough was prepared in a stand mixer (Kitchen aid®) with a dough hook kneading the flour and the water (1:1.26 w/w) for 2 min. One gram of salt was added to 300 grams of mixture. A dough ball (21.0 ± 0.58 g) was pressed with a cast iron press between polyethylene plastic sheets and was flattened with a rolling pin to the required thickness. The upper plastic was carefully peeled off, and the dough sheet was cut with a round molder of 15.24 cm in diameter. The rounded dough sheet was cooked on a laboratory hot plate at 280 °C for 70 s. Initially, each side was heated for 20 s, followed by an additional 15 s on each side. If the thin round piece of corn dough is not cooked, it remains as dried "crude" which can't be considered a genuine "tortilla." The characteristics of dried raw and dried cooked dough are quite different.

The tortillas were cooled in an atmosphere generated by a supersaturated NaCl solution prior to the drying test. Each tortilla was cut using a 10.16 cm round cutter, and the initial weight of the tortillas was recorded. The trimmed parts of the tortilla were utilized to measure the initial water content of the samples. For each test, one sample was placed right under the RJR nozzle. Then, the tortillas were dried using the impingement nozzles at different air temperatures and air mass flow rates. Two tortilla thicknesses were prepared: thin tortillas with a weight of 14.59 ± 0.65 g and thick tortillas with a weight of 18.24 ± 0.41 g.

Experimental set-up

The experimental apparatus and procedures used in this study are the same as Farzad et al.[9] Figure 1 shows the schematic of the experimental setup. The hot air was fed from a large upstream air supply to the impinging jet nozzle through a stainless-steel pipe assembly. A pressure regulator and precision gauge were mounted at the inlet to ensure constant pressure during the drying tests. The supplied compressed air, with an air temperature of 20 °C and a regulated pressure of 189.6 kPa, was utilized. The incoming air flow rate was controlled by a needle control valve and measured by a rotameter. For heating the airflow, an 8.5 kW torch electrical heater connected to a PID control unit regulated the power required to obtain the desired temperature. Following the electrical heater, a three-port solenoid valve actuated on a timer redirected the incoming air away from the sample during the sample weight recording. The threaded RJR nozzle was connected to the solenoid valve, and the impingement surface was carefully adjusted such that the centerline of the jet corresponded with the geometric center point of the surface of the samples to ensure that the impingement was symmetrical. A scale with a resolution of 0.001 g was placed under the impingement surface to record the sample weight during the drying process. An adjustable stand held the digital scale and adjusted the distance between the nozzle and the impingement surface. The weight was recorded with a data acquisition unit. J-type thermocouples were used to measure the temperatures at the outlets of the electrical heater and nozzle. Additionally, the setup was well-insulated with ceramic fiber to minimize heat loss to the ambient.

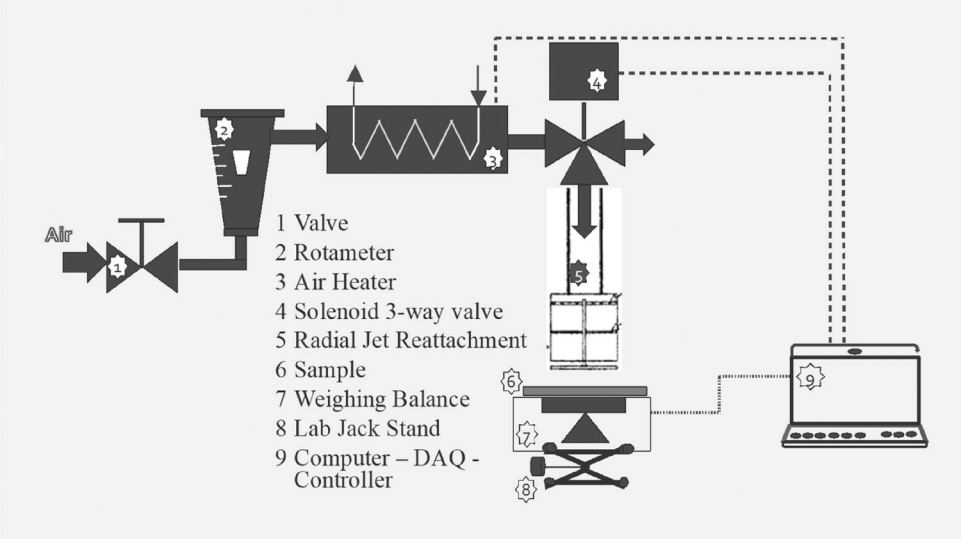

Figure 1. Experimental set-up of the RJR impingement dryer.

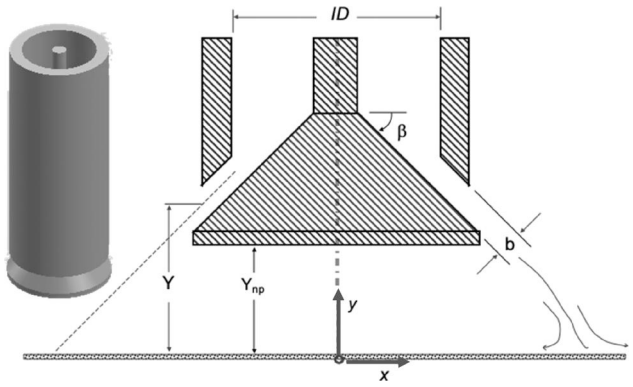

Figure 2. Perspective image (left side) and geometrical relationships (right side) of an RJR nozzle.

The geometrical relationships of the nozzles and the distance from the sample were kept constant for both of the two nozzles (Figure 2). The geometrical relationships for a single RJR nozzle recommended by Yagoobi et al.[12,19,20] were considered; b/ID = 0.145 and Ynp/ID = 0.59 (Y/Dh = 1.8). Two RJR nozzles with exit angles of 10° (inner diameter (ID) of 26.78 mm and Y of 15.80 mm) and 45° (ID of 31.81 mm and Y of 18.77 mm) were employed. The reattachment ring is the boundary or region where the flow impinges on the flat surface beneath the RJR nozzle. For both the 10° and 45° degree RJR nozzles, the selected geometrical relationship ensures that the reattachment ring takes place on the sample surface with optimal resultant averaged heat transfer coefficient. The reattachment zone is approximately a circular band with a width of 5.75 times the inner diameter of the nozzle, which allows for the airflow to cover the entire surface of the tortilla samples.

Measurement of the evaporation capacity of the system

Experimental setups are tailored for specific applications in order to measure the heat transfer performance using reattachment nozzles. The modification may involve altering the experimental setup, requiring unavailable or expensive equipment. The challenge lies in choosing the appropriate type of reattachment nozzles and determining the optimal geometrical relationship for specific applications. The evaporation capacity of an impinging RJR system can be determined by measuring the average surface temperature and the weight loss during steady-state evaporation in a saturated material. In order to do so, a porous stone immersed in a water container with the same diameter as the tortilla was used. The aluminum oxide porous stone (GSA-234 Gilson®) with a diameter of 101.60 mm, thickness of 6.35 mm, air permeability of 4.6 to 5.5 m^3/m^2 min, and an average pore size of 179 µm was used. The stone surface temperature was measured with a FLIR T540sc camera (with 2% temperature reading error).

The convective mass transfer coefficient, h_M, is calculated from the steady state evaporation rate data (flux of evaporation) Nc (kg_w/m^2 s) and the surface temperature of the wet porous stone (Ts).[21] The moisture evaporation rate can be described in terms of the averaged gas mass transfer coefficient (h_M) and the difference in moisture content between the saturated air at the surface temperature (Ys), and the mainstream moisture content (Y_G).

$$Nc = -\frac{1}{A}\frac{dW}{dt} = h_M \cdot (Y_s - Y_G) \quad (1)$$

The evaporation flux, Nc, is associated with the heat flux, q_c. The thermal energy transferred at the surface through convection enables the calculation of the averaged convective heat transfer coefficient, h_H, as follow:

$$Nc \cdot \Delta H_v = q_c = h_H \cdot (T - T_s) \quad (2)$$

The supplied compressed air is dry, with a dew point of −40 °C, at room temperature. Consequently, the gas in the mainstream is considered dry, with a moisture content approximately equal to 0 ($Y_G \sim 0$).

The mass and heat transfer coefficients are calculated based on the experimental measurements using the following equations:

$$h_M = -\frac{1}{A \cdot Y_s}\frac{\Delta W}{\Delta t} \quad (3)$$

$$h_H = -\frac{\Delta H_v}{A \cdot (T - T_s)}\frac{\Delta W}{\Delta t} \quad (4)$$

Experimental drying design

Four factors were evaluated in the impingement drying of tortillas: air temperature, air mass flow rate, nozzle type, and tortilla thickness. Two RJR nozzles were tested, one with an exit angle of 10° and the other with an exit angle of 45°. Two thicknesses of tortillas were examined: 1.03 ± 0.095 mm and 1.66 ± 0.061 mm (measured before drying), with an initial tortilla diameter of 101.6 mm. Two drying air temperatures (200 °C and 250 °C) and two levels of airflow, 17.0 m^3/h (10 CFM) and 27.2 m^3/h (16 CFM) were employed, corresponding to an air mass flow rate ($\dot{m}$) of 0.0057 kg/s and 0.0091 kg/s. The air mass flux (G) considers the tortilla surface as the impingement area for heat and mass transfer. The two air mass flux values were measured as 0.70 kg_a/m^2s and 1.12 kg_a/m^2s.

An experimental design using a complete 2^4 factorial was used, conducting three tests for each combination of variables. The evaporation rate, surface temperature, convective heat and mass transfer coefficients were considered as response variables to evaluate the evaporation capacity of the impingement nozzles. Drying time and effective diffusivity were used to evaluate the drying rate. Color and texture parameters were used to evaluate the quality characteristics of the dried tortillas. The effects of the factors on the dependent variables were evaluated using analysis of variance (ANOVA), taking into account the statistical significance at an acceptable probability level of $\alpha \leq 0.05$. The statistical analyses were conducted using with NCSS 9 software (NCSS Statistical Software, Kaysville, Utah, USA).[22]

Experimental drying kinetics

The moisture content of the tortillas before the drying tests and before the quality test was determined by weight loss of the samples after drying for over 24 h in a vacuum oven at 70 °C under a pressure of 18 kPa (method 934.06 AOAC2019).[23] Before the drying process, the trimmed parts of the tortilla were used to measure the initial water content of the samples. The initial average water content (X_{owb}) was 0.36 ± 0.023 kg_w/kg_{ws} for thin samples and, 0.42 ± 0.06 kg_w/kg_{ws} for thick samples.

The moisture content of the samples during the drying process was calculated by using the initial moisture content data and the measured weight as follow:

$$X_t = \frac{W_t}{W_o \cdot (1 - X_{owb})} - 1 \quad (5)$$

A dimensionless moisture ratio MR was used to compare the drying performance at different conditions. The moisture content at equilibrium was considered zero due to the high air temperatures used in the experiments. GRG Nonlinear solving method (Solver Add-in in Excel®) was used to fit the drying curves to an exponential-type equation (Equation (6)). The exponential equation with three adjustment parameters (B, C, and E) was used for fitting the moisture loss and drying rate curves under all the studied conditions.

$$MR = \frac{X_t - X_e}{X_o - X_e} = \frac{X_t}{X_o} = B \cdot e^{-C \cdot t^E} \quad (6)$$

The derivative of the exponential equation was used as an adjustment equation to the experimental data of drying rate.

Moisture diffusion is considered the main mechanism for mass transport inside the tortillas. The solution to Fick's second law for diffusion in a non-stationary state relates the moisture ratio (MR) to a "constant" effective moisture diffusivity (D_{eff}) as follows:[24]

$$MR = \frac{8}{\pi^2}\sum_{n=0}^{\infty}\frac{1}{(2n+1)^2}\exp\left[-(2n+1)^2\frac{\pi^2}{4}\frac{D_{eff}}{l^2}t\right] \quad (7)$$

A linearized expression, Equation (8), is obtained by considering the first term of the sum in the equation ($n = 0$). The slope of the Ln MR versus t plot is related to the diffusivity and the thickness of

the sample.

$$\ln\left[\frac{X_t - X_e}{X_o - X_e}\right] = \ln\left(\frac{8}{\pi^2}\right) - \left(D_{eff}.\frac{\pi^2}{4l^2}\right).t \qquad (8)$$

Quality measurement

The moisture content, thickness, and diameter of the tortillas were measured both before and after drying, as well as before measuring the quality parameters. More than 5 points in each tortilla piece were measured with a Dial thickness gauge of 0-5 cm (0.0025 mm graduations).

Color measurement

The CIE $L^*a^*b^*$ color coordinates were obtained with a Hunter Lab Mini Scan EZ spectrophotometer (MSEZ1118), illuminating D65. The results were expressed as CIELAB coordinates that define color in a three-dimensional space: L^* (brightness), a^* (+red, −green), b^* (+yellow, −blue), and the whiteness index, Equation (9).

$$\mathrm{WI} = 100 - \sqrt{(L^* - 100)^2 + (a^*)^2 + (b^*)^2} \qquad (9)$$

Texture analysis

The dry tortillas were subjected to a compression test until the breaking point. The physical characteristics of texture, such as hardness (*N*), crunchiness (*Nmm*), and crispiness, were calculated with the single compression graphs.[25] The compression test was performed with a TA1 texture analyzer (Lloyd Instruments AMETEK®). This texturometer was equipped with a load cell of 500 N and a stainless-steel ball probe of 1.0 cm in diameter. The sample was compressed by the probe with a preload/stress of 0.05 N, and the compression speed was set at 1 mm/s before, during, and after the test. The samples were placed over an acrylic cylindrical sample container of 5.1 cm ID and 6.35 cm OD.

Results and discussion

Heat and mass transfer at a constant evaporation rate

Table 1 shows the measured values of water evaporation rate (Nc), average surface temperature (Ts), and the calculated values of convective heat and mass transfer coefficients. The statistical analysis ($\alpha \leq 0.05$) shows that the air mass flow rate significantly affects the evaporation rate, followed by the air temperature and the nozzle type. The highest evaporation rate was 33.30 kg/m^{2}s for the 45° nozzle with temperature and air mass flow rate of 250 °C and 27.2 m^3/h, respectively. The lower evaporation rate was 16.04 kg/m^{2}s for the 10° nozzle at temperature and air mass flow rate of 200 °C and 17.0 m^3/hr, respectively. The 45° nozzle exhibited a higher evaporation rate compared to the 10° nozzle. Overall, by increasing the nozzle exit angle, force and heat transfer coefficients were increased.[12]

The average equilibrium temperatures on the surface of the porous stone ranged from 37 °C to 47 °C, with lower temperature observed for the 10° nozzle compared to the 45° nozzle. Greater flow force could cause greater surface heating.

The mass flux of the air (*G*) affected significatively ($\alpha \leq 0.05$) the average mass transfer coefficient (h_M). The values of h_M are comparable to the rate at which water evaporates from a wet surface at high air velocity (0.095 kg/m^2 s at 16 m/s).[21]

The air mass flow rate and the nozzle type are significant factors ($\alpha \leq 0.05$) in the heat transfer. Farzad et al.[9] determined the average local heat transfer coefficients of the 45° RJR nozzles by integrating the values along the boundary of a 100 mm bottom plate radius. For a similar air mass flow rate of 0.005 kg/s and an air temperature of 200 °C, an integral mean value of the heat transfer coefficient (h_H) of 32.5 W/m^{2}K was obtained compared to 26.12 W/m^{2}K in this work. The difference can be explained by the measurements in this work considered simultaneous mass and heat transfer, and the measurements made by Farzad et al. considered the heating of a metal

Table 1. Experimental convective evaporation parameters.

RJR	*G* kg m^{-2} s^{-1}	*T* °C	*Nc* (10^{-4}) kg m^{-2} s^{-1}	*Ts* °C	h_M (10^{-3}) kg_w m^{-2} s^{-1} (kg_w^{-1} kg_{da})	h_H Wm^{-2} K^{-1}
45°	1.12	250	33.30 ± 0.27	47.5	44.47	39.29
		200	27.14 ± 0.95	46.0	39.44	42.16
	0.70	250	22.20 ± 0.54	46.0	32.27	26.04
		200	17.27 ± 0.57	41.0	33.40	26.12
10°	1.12	250	29.60 ± 0.57	47.0	40.66	34.86
		200	22.70 ± 0.34	42.5	40.24	34.60
	0.70	250	18.50 ± 0.45	42.6	32.63	21.42
		200	16.04 ± 0.19	37.0	39.11	23.75

surface reaching higher temperatures than evaporative cooling.

The results obtained in this study support the use of the steady-state evaporation method as a reliable alternative to measuring heat transfer using a heat flux sensor.

Impingement drying of tortilla

Figures 3 and 4 show the drying curves at different conditions. The thickness values are those of the beginning of drying. The drying curves observed in this study align the expected order of the impact of each drying condition, namely thickness, air temperature, air mass flow rate, and nozzle type. The error bars show a greater dispersion in the tests with higher air temperatures and flow. The relationship between moisture content and time for all the drying conditions (Table 2) is well captured by the three-parameter exponential equation. The equation exhibits a sum of squared differences (SSE) of less than 0.008 and a coefficient of determination (R-squared) greater than 0.998, indicating a good fit.

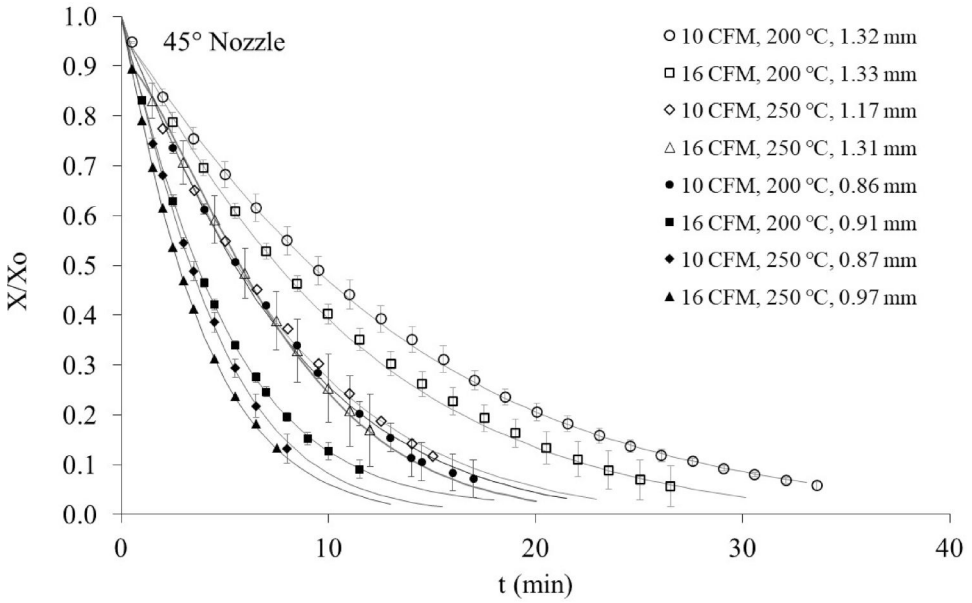

Figure 3. Tortilla drying curves with 45° nozzle. Lines are the data trend fitted by an exponential function.

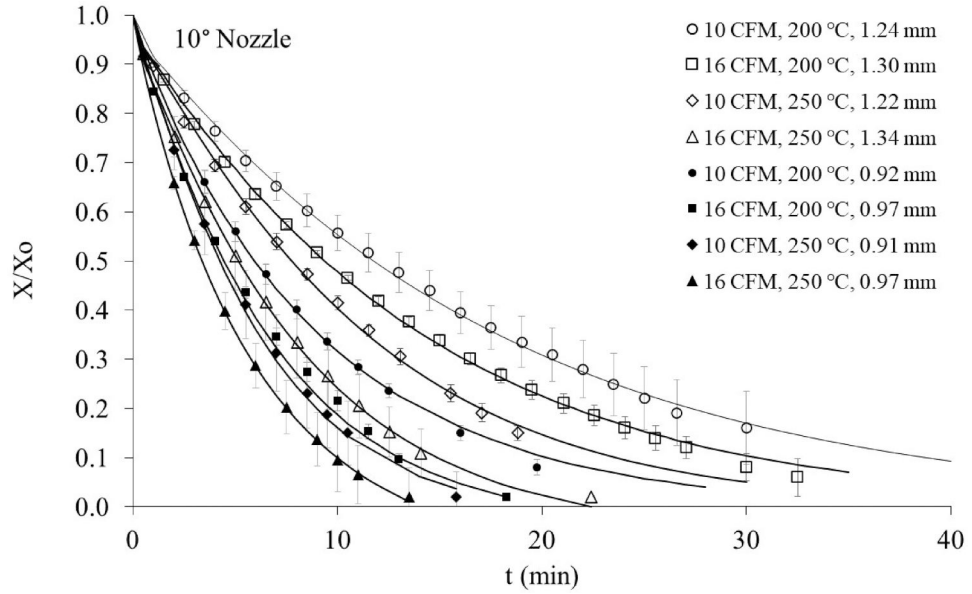

Figure 4. Tortilla drying curves with 10° nozzle. Lines are the data trend fitted by an exponential function.

Table 2. Experimental drying parameters.

						Exponentials adjustment parameters			
RJR	T °C	G $kg_a\ m^{-2}\ s^{-1}$	THK[a] mm	Nc[b] (10^{-4}) $kg_w\ m^{-2}\ s^{-1}$	t_d min	B	C min^{-e}	E	D_{eff} (10^{-10}) $m^2\ s^{-1}$
45°	250	1.12	0.97	13.51	8.50	1.000	0.233	1.067	17.11
		0.70	0.88	11.52	9.00	0.983	0.163	1.183	12.57
	200	1.12	0.91	11.66	11.00	0.984	0.161	1.116	11.79
		0.70	0.87	7.68	15.50	0.976	0.096	1.131	6.37
	250	1.12	1.31	13.40	13.53	0.918	0.052	1.405	15.14
		0.70	1.17	13.68	16.43	0.730	0.976	1.103	11.31
	200	1.12	1.33	11.31	22.53	0.971	0.073	1.090	10.84
		0.70	1.32	10.91	28.10	0.964	0.058	1.092	8.58
10°	250	1.12	0.89	12.11	10.00	0.991	0.197	0.981	13.93
		0.70	0.91	9.95	12.00	0.976	0.129	1.131	9.82
	200	1.12	0.97	9.54	13.00	0.973	0.129	1.084	9.55
		0.70	0.92	8.93	19.80	1.000	0.120	0.978	6.43
	250	1.12	1.33	12.47	14.60	0.955	0.104	1.099	16.85
		0.70	1.23	11.32	23.50	0.964	0.067	1.114	8.80
	200	1.12	1.30	10.06	30.00	0.964	0.063	1.050	8.16
		0.70	1.24	9.10	38.00	0.964	0.051	1.037	5.64

[a]After drying. [b]Evaporation rate at the beginning of the drying.

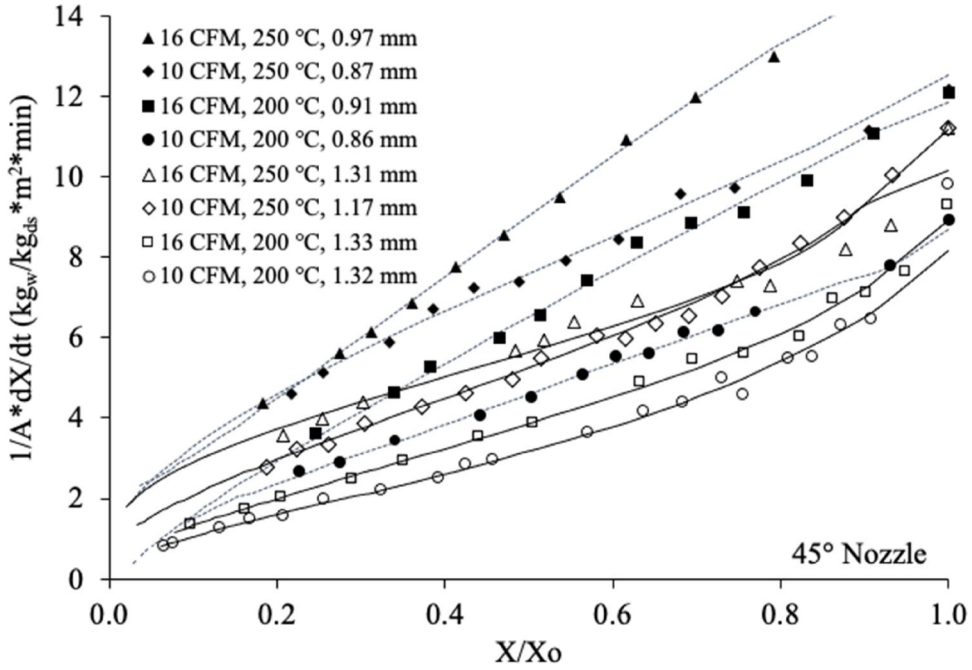

Figure 5. Drying rate using 45° nozzles. Symbols represent experimental data. The line represents predicted data with an exponential equation.

The required drying time to reach a moisture content of 0.1 kg_w/kg_{ds} is shown in Table 2. All the factors studied have a significant ($\alpha \leq 0.05$) impact on the drying time. The thickness of the product has a significant impact, followed by air temperature, airflow, and the type of nozzle. The drying time is lower for the 45° nozzle compared to the 10° nozzle. The shortest drying time of 8.5 min was achieved with more intense drying conditions (250 °C, 0.0091 kg/s), while the longest drying time of 38 min resulted with less intense conditions (200 °C, 0.0057). The drying time can be reduced more than four times with more intensive drying conditions.

The drying rates in tortillas are shown in Figure 5 for the 45° nozzle and in Figure 6 for the 10° nozzle. The drying rate using the 45° nozzle is higher than the 10° nozzle. According to these figures, thickness was the operating parameter that most influenced drying rate, followed by air temperature, air mass flow rate, and nozzle type. The exponential type equation fits the data (parameter adjustments values not shown) with a coefficient of determination R-squared more than 0.98. There is not a constant drying rate period. For the drying rate, the air temperature has a stronger impact compared to the air mass flow rate, while for the steady state evaporation rate, the air

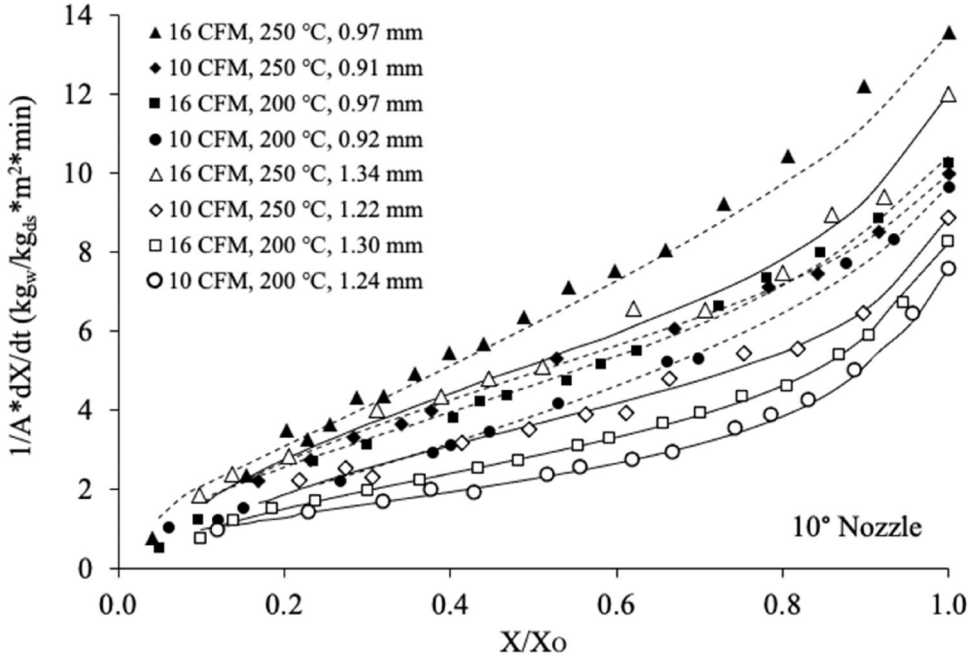

Figure 6. Drying rate using 10° nozzles. Symbols represent experimental data. The line represents predicted data with an exponential equation.

mass flow rate has a stronger impact compared to the air temperature. The evaporation capacity of the RJR Impingement (Table 1) is more than twice the initial evaporation (Table 2) of the drying of tortillas. Since the evaporation and the moisture diffusion occur simultaneously in an unsteady state, it is not feasible to calculate the evaporative capacity of the radial jet reattachment nozzles using the evaporation of the water from the tested tortilla.

The air temperature and mass flow rate significantly ($\alpha \leq 0.05$) impact effective diffusivity (Table 2). The thickness of the tortillas used does not influence the diffusivity, as expected, since the diffusivity calculation considers the material's thickness. The values with a magnitude order of 10^{-10}, indicate that diffusion inside the tortilla is not high, unless the intensive conditions (high air temperature and flow) used in impingement drying. The diffusivity is a transport parameter characteristic of the materials, which explains why the cooked tortillas dry slower than the raw tortillas (uncooked dough) according to the work of Braud et al.[24] based on the data collected by Li et al.[26]

The heat transfer Biot number (Bi_H) shows the ratio of the conductive resistance within a body to the convective resistance on the exposed surface of the body. Consequently, it considers the temperature drop inside the body to the temperature difference between the body surface and the bulk fluid. In Bi_H numbers (not shown) calculation, the steady–state heat transfer coefficients (Table 1) and the thermal conductivities of the tortillas were used. Moreira et al.[27] showed that the values of thermal conductivity of tortilla chip (0.356 water content wet basis) measured at 25 °C is 0.23 ± 0.02 W/m K. The Bi_H numbers are greater than 0.085, which means that temperature gradients across the thickness of the tortilla can increase as the tortilla dehydrates, ($Bi_H > 0.1$). The mass transfer Biot number (Bi_M) values (not shown) calculated using the mass transfer coefficients (Table 1) and, the effective moisture diffusivities (Table 2) are higher than 3400; thus, the internal resistance to mass transfer cannot be neglected and the moisture concentration gradients are not uniform along of the thickness of the tortilla ($Bi_M > 0.1$).[28]

Quality of the tortilla dried by impingement

The shrinkage of the tortilla pieces is similar for all the drying conditions. The dried tortillas shrank by 7.17% from their initial diameter, with a final average diameter of 9 cm. The thickness reduction is about 14% for thin and 22.6% for thick tortillas. The decrease in diameter is more remarkable in dehydrated raw tortillas[7] (10% and 14%) than in dry cooked tortillas.

The color parameter and texture quality of impinging drying tortilla are presented in Table 3. For comparison in terms of the dried product quality, the

Table 3. Color and texture of impingement dried tortillas.

				Color				Texture		
RJR	T °C	$\dot{m}$ g s^{-1}	*THK* mm	L^*	a^*	b^*	*WI*	Hardness (*N*)	Crunchiness (*Nmm*)	Crispiness
45°	250	9.1	0.97	68.06	2.60	23.68	60.10	16.40	53.35	39.51
		5.7	0.88	66.58	2.29	23.18	59.25	16.84	56.19	45.84
	200	9.1	0.92	67.42	2.77	24.21	59.31	13.34	39.95	42.86
		5.7	0.87	68.36	3.15	24.27	59.97	13.24	42.09	39.03
	250	9.1	1.31	72.48	2.69	24.55	63.02	21.86	72.25	71.22
		5.7	1.17	66.47	2.03	24.05	58.69	23.91	86.76	76.39
	200	9.1	1.33	67.51	2.47	24.33	59.33	27.39	48.44	69.70
		5.7	1.32	67.68	2.34	22.97	60.28	25.53	72.61	84.85
10°	250	9.1	0.98	66.49	2.14	24.33	58.52	17.44	40.06	38.37
		5.7	0.91	68.26	2.12	23.52	60.44	15.16	50.34	46.76
	200	9.1	0.97	65.88	2.42	23.45	58.52	14.51	51.01	37.28
		5.7	0.92	65.40	2.64	24.45	57.52	13.18	61.77	34.66
	250	9.1	1.33	68.58	1.87	22.85	61.11	25.49	68.13	87.23
		5.7	1.23	68.14	1.70	22.63	60.88	25.38	68.26	80.46
	200	9.1	1.30	67.45	2.09	23.59	59.74	27.57	48.59	68.97
		5.7	1.24	67.09	1.91	22.55	60.06	26.31	52.12	79.56
Handmade unfried tostadas			2.77	75.41	1.16	20.70	67.52	21.12	62.17	74.47

color and texture of artisanal prepared dried tortillas (handmade unfried tostadas) are included in Table 3.

The color of the tortillas changes from cream to beige after the impingement drying. The color was uniform throughout the piece of dehydrated tortillas. The whiteness index is the parameter that better assessed the effect of drying conditions on the color. Somewhat higher Whiteness Index values are observed at higher temperatures and airflow, possibly due to intensive drying conditions. The artisanal dried tortillas, have a higher whiteness than those dried using the RJR nozzles. Neither the thickness nor the exit angle of the RJR nozzle affects the final color of the dehydrated tortillas. The drying conditions and the type of nozzle studied do not show a significant effect ($\alpha \leq 0.05$) on the color.

The effect of the thickness on the texture parameter is evident (Table 3). The cooked tortillas dried with RJR nozzles are three times less fragile than those raw tortillas impinging dried studied by Lujan et al.[7] The texture characteristics of the artisanal dry tortillas are similar to tortillas dried with RJR nozzles, even though the thickness of the former is greater. The thermic treatment differences of each process affect the microstructure and texture of the dried product.[7] Special care was taken in the preparation of the samples, as indicated by the methodology, so that all the tortillas used in the tests were similar. With the operating conditions explored in this study, no bubbles or deformations were observed and the initial roughness of the tortilla did not change during dehydration.

Cross effects on texture parameters are presented concerning the type of nozzle used. For the 10° nozzle, hardness increases, and crunchiness decreases with increasing air temperature and flow. For the 45° nozzle, hardness and crunchiness increase at high air temperatures and flow. The statistical analysis shows that neither the type of nozzle nor the drying air conditions studied significantly ($\alpha \leq 0.05$) affect the final product's texture. This means that it is possible to have a robust process of impinging drying tortillas in which the variation of the process conditions or disturbances do not significantly impact the quality characteristics of the final product offered to the consumer.

Conclusions

The experimental measurement of the steady-state evaporation rate was a simple way to assess the heat and mass transfer of a complex device like the RJR nozzle. This method can help define and establish the best geometrical relationships of different kinds of nozzles with other operational conditions for specific applications, like food impingement drying.

The evaporation rates were different for the two RJR nozzles. Thus, the exit angle of the RJR nozzle impacted the drying time of the tortillas. The drying rate using the RJR 45° was higher than that using the RJR nozzle with an exit angle of 10°. Unless intensive air conditions and high heat transfer devices were used, the diffusion inside the tortilla (10^{-10}) was not high, as this property depended on the structural characteristics and the effect of the conditions in the material. Convection and diffusion should be considered in impinging drying of food.

The Impingement drying of tortillas using an RJR nozzle is a promising method for producing crispy (unfried) tostadas. Similar color and texture characteristics of handmade (unfried) tostadas and those dried using RJR nozzles were obtained for all drying conditions evaluated.

Impinging drying with RJR nozzles is a viable and robust technology that can be integrated into the tortilla cooking process to produce "no-fry tostadas." The drying time can be modified by changing the condition to accommodate continuous processes with conveyor belts with little change in the final quality characteristics.

Nomenclature

A	Area for heat and mass transport, m^2
B	Adjustment parameter exponential equation [—]
b	Nozzle exit opening, mm
B	Adjustment parameter exponential equation [—]
Bi_H	Heat transfer Biot number ($h_H \cdot l \cdot k_{ws}^{-1}$) [—]
Bi_M	Mass transfer Biot number ($h_M \cdot l \cdot D_{eff}^{-1}$) ($R \cdot T \cdot P^{-1} \cdot PMa^{-1}$) [—]
C	Adjustment parameter exponential equation, min^{-e}
E	Adjustment parameter exponential equation [—]
D_{eff}	Effective moisture diffusivity, m^2/s
Dh	Hydraulic diameter, mm
G	Mass flux of air, kg_{da}/m^2 s
ΔH_v	Enthalpy of vaporization, kJ/kg
h_M	Average Convective mass transfer coefficient, $kg_w/(m^2 s\ kg_w/kg_{da})$
h_H	Average Convective heat transfer coefficient, W/m^2 K
ID	Inner diameter, mm
k	Heat conductivity, W/m K
l	Thickness, m
L^*, a^*, b^*	Cielab space color coordinates
MR	Moisture ratio [—]
$\dot{m}$	Air mass flow, kg_a/s
n	Number of the summands
Nc	Evaporation rate, kg_w/m^2 s
q_c	Flux of heat, W/m^2
t	Times
t_d	Drying time to reach 0.1 kg_w/kg_{ds} min
T	Airstream temperature, °C
Ts	Surface temperature°C
THK	Thickness, mm
Y	Nozzle opening to surface spacing, mm
Ynp	Nozzle base to surface spacing, mm
Y_G	Humidity of the air at the mainstream, kg_w/kg_{da}
Ys	Saturated air humidity at Ts, kg_w/kg_{da}
W	Weight, kg
WI	Whiteness index [—]
X	Water content dry basis, kg_w/kg_{ds}
X_{wb}	Water content wet basis, kg_w/kg_{ws}

Greek letters

α	Significance
β	Nozzle exit angle

Subscripts

a	Air
da	Dry air
ds	Dried solid
e	At equilibrium
o	Initial
s	Saturated
t	Referred a time
w	Water
ws	Wet solid

Disclosure statement

No potential conflict of interest was reported by the author(s).

Funding

This study was supported by the Center for Advanced Research in Drying (CARD), a National Science Foundation Industry-University Cooperative Research Center located at Worcester Polytechnic Institute. The Rodríguez-Ramírez J. author acknowledges CONACyT of Mexico for the international scholar fellowship.

References

[1] Lujan-Acosta, J.; Moreira, R. G. Reduction of Oil in Tortilla Chips Using Impingement Drying. *LWT Food Sci. Technol.* **1997**, *30*, 834–840. DOI: 10.1006/fstl.1997.0282.

[2] Serna-Saldivar, S. O.; Rooney, L. W. Chapter 13 – Industrial Production of Maize Tortillas and Snacks. In *Tortillas*; Rooney, L. W., Serna-Saldivar, S. O., Eds.; AACC International Press, **2015**; pp 247–281 DOI: 10.1016/B978-1-891127-88-5.50013-X.

[3] Mujumdar, A. S. Chapter 16: Impingement Drying. In *Handbook of Industrial Drying*, 4th ed.; Mujumdar, A. S., Ed.; CRC Press: Boca Raton, FL, **2015**; pp 371–380.

[4] Tsotsas, E.; Mujumdar, A. S., Eds. *Modern Drying Technology, Volume 5: Process Intensification*; John Wiley & Sons: New York, **2014**.

[5] Polat, S. Heat and Mass Transfer in Impingement Drying. *Drying Technol.* **1993**, *11*, 1147–1176. DOI: 10.1080/07373939308916894.

[6] Sarkar, A.; Nitin, N.; Karwe, M. V.; Singh, R. P. Fluid Flow and Heat Transfer in Air Jet Impingement in Food Processing. *J. Food Sci.* **2004**, *69*, CRH113–CRH122. DOI: 10.1111/j.1365-2621.2004.tb06315.x.

[7] Lujan-Acosta, J.; Moreira, R. G.; Yagoobi, J. Air-Impingement Drying of Tortillas Chips. *Drying Technol.* **1997**, *15*, 881–897. DOI: 10.1080/07373939708917266.

[8] Banooni, S.; Hosseinalipour, S. M.; Mujumdar, A. S.; Taheran, E.; Bahiraei, M.; Taherkhani, P. Baking of Flat Bread in an Impingement Oven: An Experimental Study of Heat Transfer and Quality

Aspects. *Drying Technol.* **2008**, *26*, 902–909. DOI: 10.1080/07373930802142614.

[9] Farzad, M.; Ferouali, H. E.; Kahraman, O.; Yagoobi, J. Enhancement of Heat Transfer and Product Quality Using Jet Reatachment Nozzles in Drying of Food Products. *Drying Technol.* **2022**, *40*, 352–370. DOI: 10.1080/07373937.2020.1804927.

[10] Farzad, M.; Yagoobi, J. Drying of Moist Cookie Doughs with Innovative Slot Jet Reattachment Nozzle. *Drying Technol.* **2021**, *39*, 268–278. DOI: 10.1080/07373937.2020.1729173.

[11] Yagoobi, J. S.; Narayanan, V.; Page, R. H.; Wirtz, J. W. Comparison of Heat Transfer Characteristics of Radial Jet Reatachment Nozzle to in-Line Impinging Jet Nozzle. ASME1996, Proceeding of the National Heat Transfer Conference, **1996**; Vol. 2, pp 85–92.

[12] Seyed-Yagoobi, J. Enhancement of Heat and Mass Transfer with Innovative Impinging Jets. *Drying Technol.* **1996**, *14*, 1173–1196. DOI: 10.1080/07373939608917143.

[13] Page, R.; Hadden, L.; Ostowari, C. Theory for Radial Jet Reattachment Flow. *AIAA J.* **1989**, *27*, 1500–1505. DOI: 10.2514/3.10294.

[14] Narayanan, V.; Seyed-Yagoobi, J.; Page, R. An Experimental Study of Fluid Mechanics and Heat Transfer in an Impinging Slot Jet Flow. *Int. J. Heat Mass Transfer* **2004**, *47*, 1827–1845. DOI: 10.1016/j.ijheatmasstransfer.2003.10.029.

[15] Narayanan, V.; Page, R. H.; Seyed-Yagoobi, J. Visualization of Airflow Using Infrared Thermography. *Exp. Fluids* **2003**, *34*, 275–284. DOI: 10.1007/s00348-002-0557-x.

[16] Seyed-Yagoobi, J.; Narayanan, V.; Page, R. Comparison of Heat Transfer Characteristics of Radial Jet Reattachment Nozzle to in-Line Impinging Jet Nozzle. *Trans. ASME J. Heat Transfer* **1998**, *120*, 335–341. DOI: 10.1115/1.2824253.

[17] Narayanan, V.; Seyed-Yagoobi, J.; Page, R. Heat Transfer Characteristics of a Slot Jet Reattachment Nozzle. *J. Heat Transfer* **1998**, *120*, 348–356. DOI: 10.1115/1.2824255.

[18] Martin, H. Heat and Mass Transfer between Impinging Gas Jets and Solid Surfaces. *Adv. Heat Transfer* **1997**, *13*, 1–60. DOI: 10.1016/S0065-2717(08)70221-1.

[19] Narayanan, V.; Seyed-Yagoobi, J.; Page, R. H. Transient Thermal Structure, Turbulence, and Heat Transfer in a Reattaching Slot Jet Flow. *Int. J. Heat Mass Transfer* **2004**, *47*, 5219–5234. DOI: 10.1016/j.ijheatmasstransfer.2004.06.016.

[20] Wu, J.; Seyed-Yagoobi, J.; Page, R. H. Heat Transfer and Combustion Characteristics of an Array of Radial Jet Reattachment Flames. *Combus. Flames* **2001**, *125*, 955–964. DPI: DOI: 10.1016/S0010-2180(00)00251-0.

[21] Treybal, R. E. *Mass-Transfer Operations*, 3rd ed.; McGraw-Hill: London, **1981**.

[22] NCSS Version 9; NCSS Statistical Software; NCSS: Kaysville, UT, **2016**.

[23] AOAC Official Methods of Analysis. 13th ed.; Association of Official Analytical Chemists: Washington, DC, **1990**.

[24] Braud, L. M.; Moreira, R. G.; Castell-Perez, M. E. Mathematical Modeling of Impingement Drying of Corn Tortillas. *J. Food Eng.* **2001**, *50*, 121–128. DOI: 10.1016/S0260-8774(00)00234-X.

[25] Civille, G. V.; Szczesniak, A. S. Guidelines Training a Texture Profile Panel. *J. Texture Stud.* **1973**, *4*, 204–223. DOI: 10.1111/j.1745-4603.1973.tb00665.x.

[26] Li, Y. B.; Seyed-Yagoobi, J.; Moreira, R. G.; Yamsaengsung, R. Superheated Steam Impingement Drying of Tortilla Chips. *Drying Technol.* **1999**, *17*, 191–213. DOI: 10.1080/07373939908917525.

[27] Moreira, R. G.; Palau, J.; Sweat, V. E.; Sun, X. Thermal and Physical Properties of Tortilla Chips as a Function of Drying Time. *J Food Process. Preserv.* **1995**, *19*, 175–189. DOI: 10.1111/j.1745-4549.1995.tb00287.x.

[28] Bruin, S.; Luyben, K. C. A. M. Drying of Food Materials: A Review of Recent Developments. In *Advances in Drying*; Mujumdar, A. S., Ed.; Hemisphere Publishing Corporation: London, **1980**; pp 155–215.